Anion-π Interaction

Literature Seminar 07.03.17.
Shinji Harada

1. Introduction: π-Cloud of Aromatic Ring

The ability of the π-cloud of aromatic compounds to interact with positively charged atoms or the hydrogen of a hydrogen bond donor is well known.

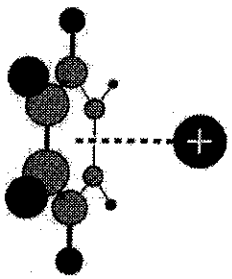

M^+	Binding Energy (kcal/mol)
Li^+	38
Na^+	28
K^+	19
Rb^+	16

Gas Phase Cation-π Interaction

–19.2 kcal/mol –9.4 kcal/mol

vs.

H_2O·····K^+ H_2O·····NMe_4^+

–17.9 kcal/mol –9.0 kcal/mol

J. Chem. Phys. **1981**, *85*, 1814.
J. Am. Chem. Soc. **1985**, *107*, 469. and 474.

Cation-π Interactions in Structural Biology

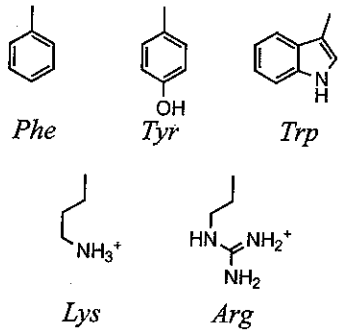

Phe *Tyr* *Trp*

Lys *Arg*

- One cation-π interaction for every 77 amino acids
- *Arg* preferred over *Lys*
- Over 25% of all tryptophans involved in a cation-π interaction

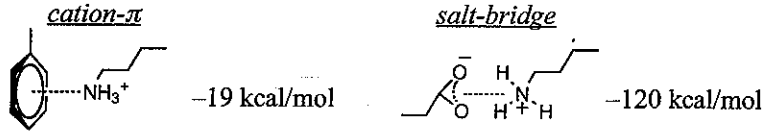

Phe *Lys* *Asp* *Lys*

J. Am. Chem. Soc. **2000**, *122*, 870.

(*hidrogen bond* : –2 ~ –10 kcal/mol)

The cation-π interaction is in general dominated by electrostatic and cation-induced polarization.

(For a review for cation-π interaction, see: Ma, J. C.; Dougherty, D. A. *Chem. Rev.* **1997**, *97*, 1303.
See also Dr.Kumagai's literature seminar (D1): January 8th, 2003.)

However, how is the case for the opposite electrostatics?

Aromatic π systems are generally considered to be electron-rich and are expected to exhibit repulsive interaction with anions....

Do anion-π interactions exist?

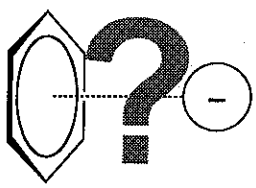

Contents

2. Anion-π Interaction: Its Nature and Examples

- The practical scope for recognition and binding of anions is considerably narrower than that for cations. Localized electron deficients involve Lewis acidic sites (organomercury, tin, boron or ammonium salt) which are less conveniently integrated into receptor design than easily manipulable heteroatom or π system.

- In early 90s, simple ion pairing of anions with ammonium centers in macrocycles has been applied both on its own and in conjunction with hydrogen bonding to the effective complexation of halides. Although macrocycles were mostly cyclophanes, the aromatic π-system did not participate in the coordination.

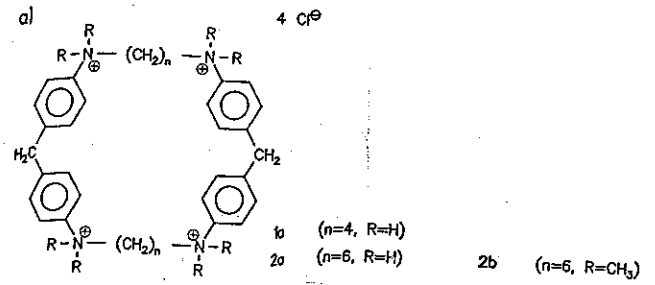

Schneider, H.-J. *et al.*
Angew. Chem. Int. Ed. Engl. **1991**, *30*, 1417.
J. Am. Chem. Soc. **1992**, *114*, 7704.

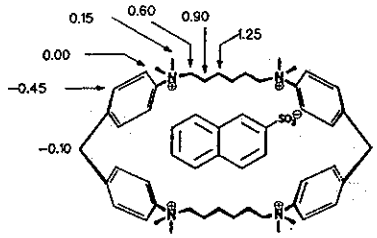

- In late 90s, there were several reports on theoretical evidence of electrostatic bonding between hexafluorobenzene and the heteroatom in molecules, like H_2O, HCN and HF.

An Attractive Interaction between the π-Cloud of C_6F_6 and Electron-Donor Atoms

J. Org. Chem. **1997**, *62*, 4687.

Ibon Alkorta,* Isabel Rozas, and Jose Elguero

Instituto de Química Médica (CSIC), Juan de la Cierva, 3, E-28006-Madrid, Spain

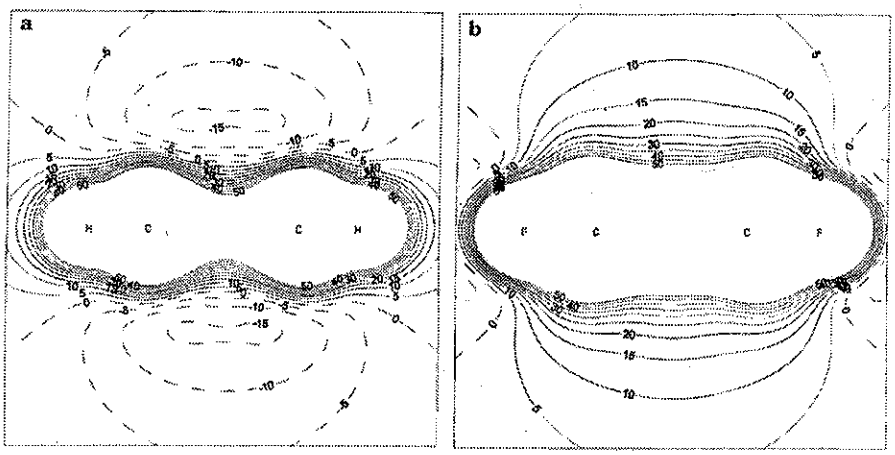

The negative end of the dipole is directed toward the C_6 axis of the ring.

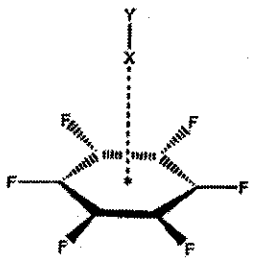

X-Y : F-H, H-Li, N≡CH
C≡NH, :CH2

Figure 3. Molecular electrostatic potential (kcal/mol) of (a) benzene and (b) hexafluorobenzene above and below the aromatic plane.

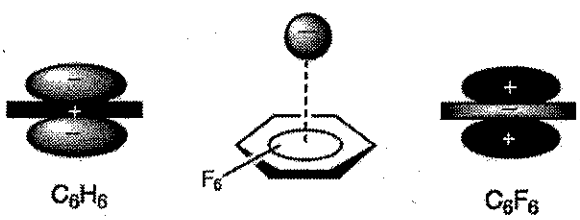

The important role of the permanent quadrupolesof the two molecules (benzene and hexafluorobenzene), which are similar in magnitude but of opposite sign.
A positive region is obtained in the case of C_6F_6.
A similar effect is expected for other aromatic compounds with a large number of withdrawing groups.

Water-Hexafluorobenzene Interaction

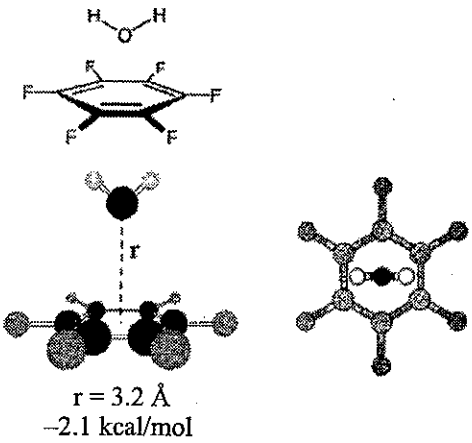

r = 3.2 Å
–2.1 kcal/mol

Danten, Y.; Tassaing, T.; Besnard, M. *J. Phys. Chem. A* **1999**, *103*, 3530.
Gallivan, J. P.; Dougherty, D. A. *Org. Lett.* **1999**, *1*, 103.

Benzene Forms Hydrogen Bonds with Water

Suzuki, S.; Green, P.G.; Bumgarner, R.E.; Dasgupta, S.; Goddard, W.A.III; Blake, G.A. *Science* **1992**, *257*, 942.

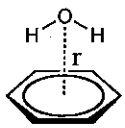

r = 3.3 Å
–1.8 kcal/mol

In host-guest chemistry, other π-deficient aromatic systems were extensively examined.

Mascal, M.; Armstrong, A.; Bartberger, M.D. *J. Am. Chem. Soc.* **2002**, *124*, 6274.
Alkorta, I.; Rozas, I.; Elguero, J. *J. Am. Chem. Soc.* **2002**, *124*, 8593.

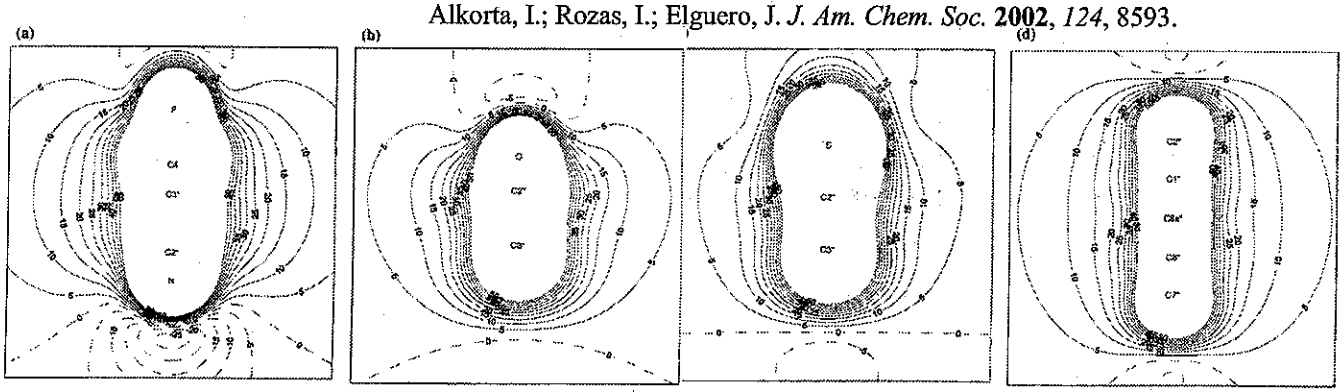

Figure 2. MEP maps (kcal/mol) of (a) C_5F_5N, (b) C_4F_4O, (c) C_4F_4S, (d) $C_{10}F_8$ in the perpendicular plane to the aromatic rings. The stars indicate that the position of the atom is projected to the plane studied. For the MEP map of C_6F_6, see ref 2.

Several perfluoro-aromatic compounds have been examined with different anions (F^-, Cl^-, Br^-, H^-, CN^-, and CH_3^-).

1,3,5-Triazine ring also associate with anions. Its quadrupole is slightly possitive.

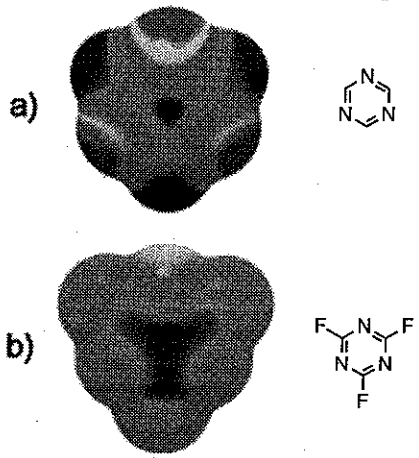

Figure 1. Calculated 6-31+G*//6-31+G* electrostatic potential surfaces for (a) 1,3,5-triazine and (b) trifluoro-1,3,5-triazine. Electrostatic potential surface energies range from −15 (red) to +15 (blue) kcal mol^{-1} for 1,3,5-triazine and −35 (red) to +35 (blue) kcal mol^{-1} for trifluoro-1,3,5-triazine.

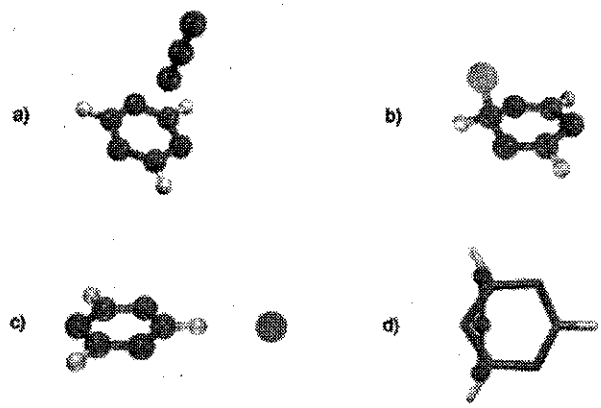

Figure 2. Modeled representations of (a) the triazine–azide aryl centroid complex **3c**; (b) the triazine–fluoride "attack" complex **5b**; (c) the triazine–chloride H-bonding complex **7a**; and (d) the triazine–azide "stack" complex **8**.

Theoretical Investigation

A powerful tool for predicting the binding properties of aromatic compounds: **MIPp**
Molecular Interaction Potential with polarization (Luque, J.F.; Orozco, M. *J. Comput. Chem.* **1998**, *19*, 866.

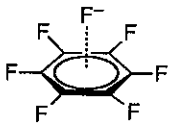

(r = 2.6 Å)

Calculation of MIPp of hexafluorobenzene interaction with F^-.
The results in Table 2 point out the importance of the polarization (induction) component, which is similar to the electrostatic one in 2.0-3.0 Å range.

Table 2. Contributions to the total interaction energy [kcalmol^{-1}] calculated with MIPp for hexafluorobenzene interacting with F^- at several distances [Å] from the center of the ring.

Distance	E_e	E_p	E_{vw}	E_t
1.5	−36.59	−43.84	1047.82	967.38
2.0	−22.44	−24.89	119.05	71.72
2.5	−16.39	−13.93	13.44	−16.89
3.0	−12.66	−7.96	−0.50	−20.12
3.5	−9.90	−4.74	−0.83	−15.48

E_e : electrostatic, E_p : polarization, E_{VW} : van der Waals, E_t : total

Angew. Chem. Int. Ed. **2002**, *41*, 3389.

The electrostatic interaction arises from the interaction of the quadrupole moment of π system with the anion. The induction energy can be described by the polarization of molecule due to shifts of electron in the direction of the electronegative group.

Total interaction energies of anion-π complex is comparable to that of the corresponding cation-π complex !!

Other kinds of π systems (olefin and heteroaromatics) were also investigated.

Kim, D.; Tarakeshwar, P.; Kim, K.S. *J. Phys. Chem. A* **2004**, *108*, 1250.

Garau, C.; Frontera, A.; Quiñonero, D.; Ballester, P.; Costa, A.; Deyà, P.M. *J. Phys. Chem. A* **2004**, *108*, 9423.

Besides electrostatic interaction and induction energy, dispersion forces play an important role in the anion-π interaction. Dispersion interaction could be attributed to the MO interaction between anion and π system. (HOMO of anion and LUMO of π system). This is due to the high electron density and large ionic radii of halide anions.

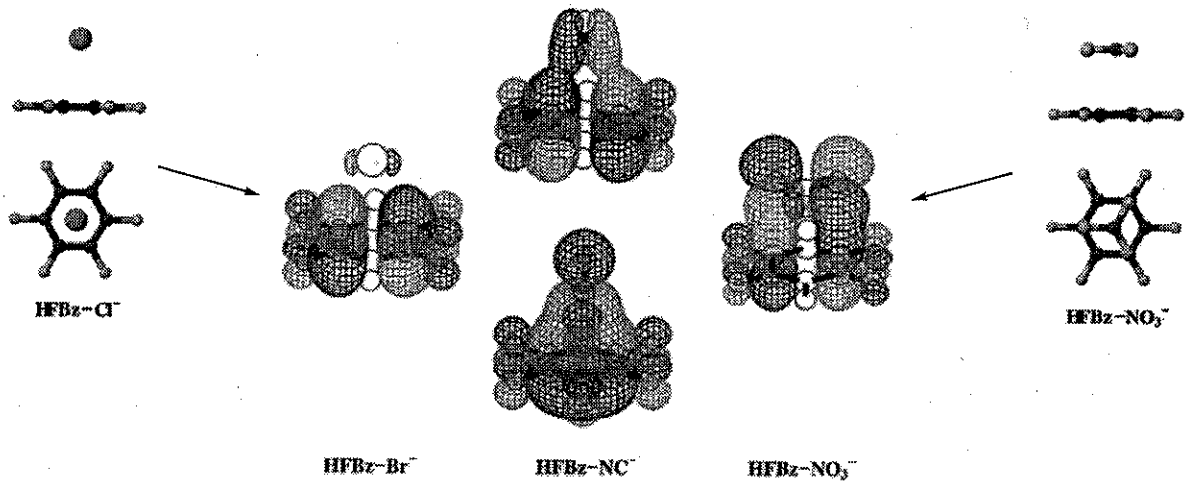

Figure 5. Representative dispersive type of molecular orbital interactions between the highest occupied orbitals of anions and those of C_6F_6. The left one is for the complex of Br^-, the middle ones are for that of NC^-, and the right one is for that of NO_3^-.

Glossary of Terms

- **Electrostatic potential** - A physical property equal in magnitude to the electrostatic energy between the static charge distribution of an atomic or molecular system (in the latter case the term molecular electrostatic potential is commonly used) and a positive unit point charge located at r.
- **Dispersion energy** - An attractive component of the energy of intermolecular interaction resulting from the interaction between the instantaneous, time-variable dipole of one system and the induced multipole of the second system.
- **Inductive effect (polarization)** - The polarization of chemical bonds due to shifts of their electron pairs in the direction of the electronegative group. Within a molecule, the inductive effect is transmitted through space and is determined by electrostatic forces between the interacting sites. Another original model of inductive effect relates to through-bond transmission by successive polarization of the bonds between a dipolar or charged substituent and the reaction site.
- **Exchange repulsion** - The correction to the Coulomb repulsion between two electrons in orbitals for the case when the electrons possess parallel spins.
- **Correlation energy** - The difference between the energy of a system calculated as the minimal value within the Hartree-Fock approximation and the exact non-relativitistic energy of that system.
  The correlation energy arises because the Hamiltonian in the Hartree-Fock method includes an averaged interelectronic potential which does not account for the electron correlation in a molecular system.
- **Hartree-Fock (Self-Consistent Field, SCF) method** - Method for determination of the spatial orbitals of the many-electron determinantal wavefunction based on reducing coupled nonlinear differential equations for the optimum forms of the molecular orbitals by use of the variational method. The Hartree-Fock hamiltonian operator is defined in terms of these orbitals through the operators of coulomb and exchange repulsion.
  The general procedure for solving the Hartree-Fock equations is to make the orbitals self-consistent with the potential field they generate. It is achieved through an iterative trial-and-error computational process, for which reason the entire procedure is called the self-consistent field method.

for more precise explanation, see: IUPAC Home Page. URL: http://www.iupac.org/reports/1999/7110minkin/

Lone Pair-π Interaction

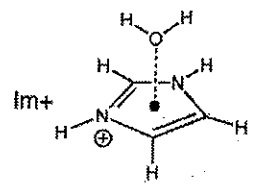

ΔE = -9.778; dπ = 2.93 (MP2/6-31G*)

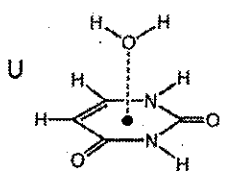

ΔE = -3.338; dπ = 2.85 (MP2/6-31G*)

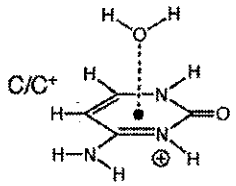

ΔE(C) = -2.813; dπ = 3.13 (MP2/6-31G*)
ΔE(C+) = -9.954; dπ = 2.72 (MP2/6-31G*)

Water–Nucleobase "Stacking": H–π and Lone Pair–π Interactions in the Atomic Resolution Crystal Structure of an RNA Pseudoknot

Sanjay Sarkhel,[†] Alexander Rich,[‡] and Martin Egli*,[†]

J. Am. Chem. Soc. **2003**, *125*, 8998.

A

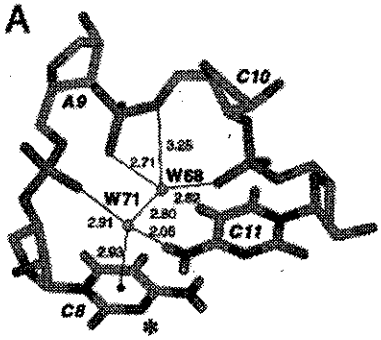

RNA pseudoknot
from beet western yellow virus

C

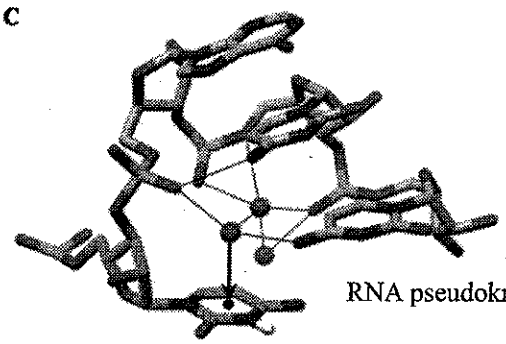

RNA pseudoknot from Potato Leaf Roll Virus

Water sit on top of a functionally important, protonated cytosine in the crystal structure (indicated by an arrow).

3. Anion-π Interaction in Metal Complexes

Cambridge Structural Database (CSD) is a convenient and reliable storehouse for geometrical information.

"Crystal structures are so rich in information and often reveal effects that had not been noticed by the original authors."

Quiñonero, D.; Garau, C.; Rotger, C.; Frontera, A.; Ballester, P.; Costa, A.; Deyà, P.M. *Angew. Chem. Int. Ed.* **2002**, *41*, 3389.

Figure
Plots obtained directly from analysis of CSD for structures where noncovalent interactions are present between an electronegative atom (F, Cl, Br, O, S, and N) and a perfluorobenzene fragment.

a) The number of structures obtained at an angle defined by the electronegative atom, the ring centroid, and one C atom of the ring.
b) Scatterplot for the structures where the same angle and the average of all six X-C distances.

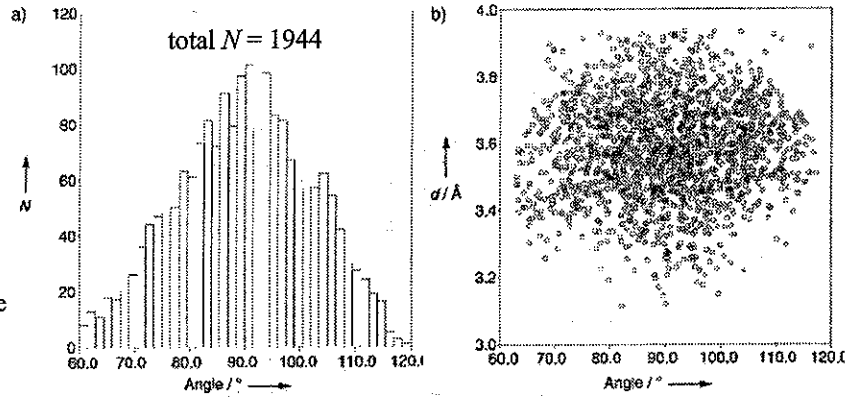

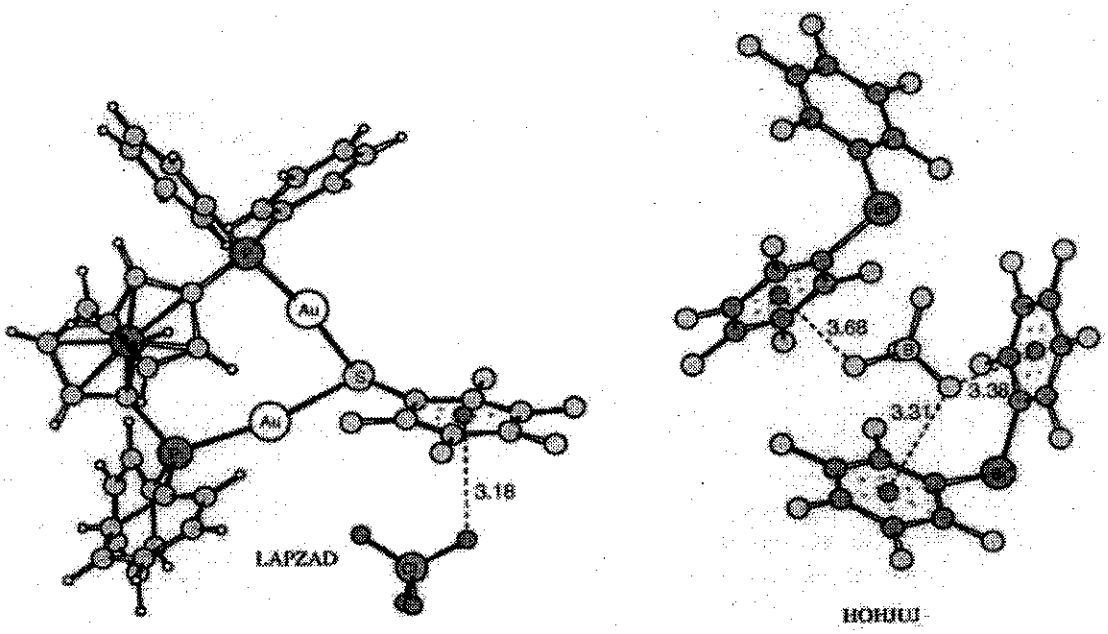

Figure 3. X-ray crystal structures of $[(Ph_2PC_5H_4)_2FeAu_2SC_6F_5][ClO_4]$ (LAPZAD)[31] and $[(C_6F_5)_2Br][BF_4]$ (HOHJUJ); distances in Å.

Anion–π Interactions in a Carousel Copper(II)–Triazine Complex

Serhiy Demeshko, Sebastian Dechert, and Franc Meyer*

J. Am. Chem. Soc. **2004**, *126*, 4508.

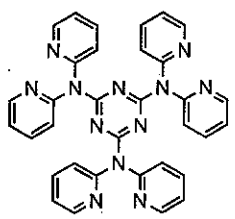

+ 3 $CuCl_2$

hexakis(pyridin-2-yl)-[1,3,5]-triazine-2,4,6-triamine

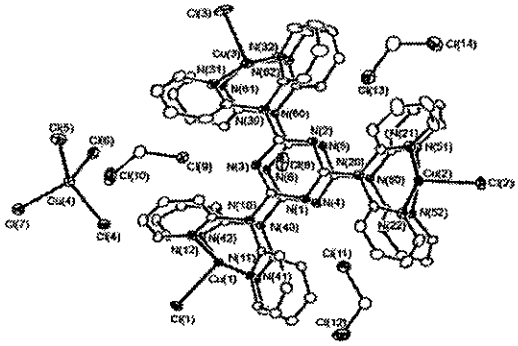

Figure 1. Structure of **2** (ORTEP; 30% probability thermal ellipsoids). All hydrogen atoms, two CH_2Cl_2, and CH_3OH are omitted for clarity. Selected bond lengths [Å]: Cu(*n*)–Cl(*m*), 2.382(1)–2.407(1) (*n* = *m* = 1–3), 2.238(1)–2.261(1) (*n* = 4, *m* = 4–7); Cu(*n*)–N, 2.025(4)–2.044(4) (*n* = 1), 2.022(4)–2.037(4) (*n* = 2), 2.016(4)–2.036(4) (*n* = 3).

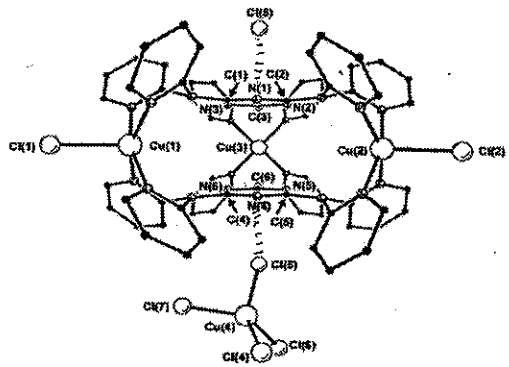

Figure 2. Emphasis of the position of the chlorine atoms Cl(8) and Cl(5) in relation to the cationic $[L_2(CuCl)_2]^{3+}$ moiety of **2**. Distance from Cl(8) to [C(1)–N(3)] mean plane, 3.166(2) Å, and from Cl(8) to [C(1)···N(3)] ring centroid, 3.170(2) Å; ring-slippage, 0.163 Å. Angle of the Cl(8)···[C(1)···N(3)] centroid axis to the plane of the ring [C(1)···N(3)], 87.1(1)°. Distance from Cl(5) to [C(4)···N(6)] mean plane, 3.109(2) Å, and from Cl(5) to [C(4)···N(6)] ring centroid, 3.112(2) Å; ring-slippage, 0.118 Å. Angle of the Cl(5)···[C(4)···N(6)] centroid axis to the plane of the ring [C(4)···N(6)], 87.8(1)°.

Structural Criteria for the Design of Anion Receptors: The Interaction of Halides with Electron-Deficient Arenes

Orion B. Berryman,[§] Vyacheslav S. Bryantsev,[†] David P. Stay,[§] Darren W. Johnson,*[,§] and Benjamin P. Hay*[,†]

J. Am. Chem. Soc. **2007**, *129*, 48.

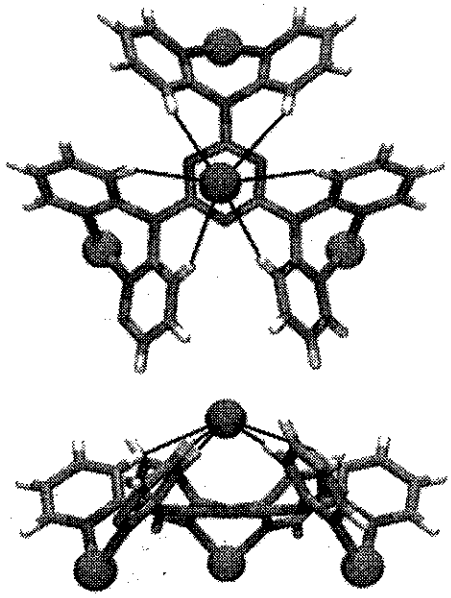

Figure 1B. Views of a fragment of a Cl^- receptor[15] crystal structure showing six hydrogen-bonding interactions with aryl C–H groups of Cu(II)-coordinated pyridine rings and one anion–π interaction with a melamine ring. Interaction geometries are near ideal with all C–H···Cl^- angles ≥ 150° and Cl^- to C distances ranging from 3.9 to 4.3 Å.

An Aromatic Anion Receptor: Anion–π Interactions do Exist**

Angew. Chem. Int. Ed. **2004**, *43*, 5815.

Paul de Hoog, Patrick Gamez, Ilpo Mutikainen, Urho Turpeinen, and Jan Reedijk**

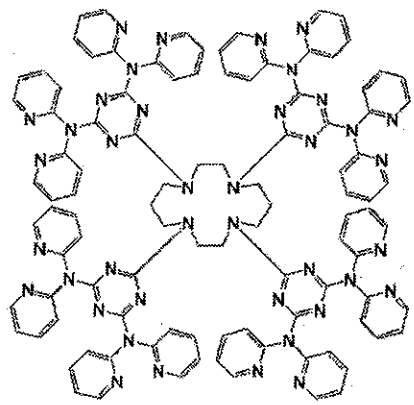

azadendtriz

$CuCl_2$

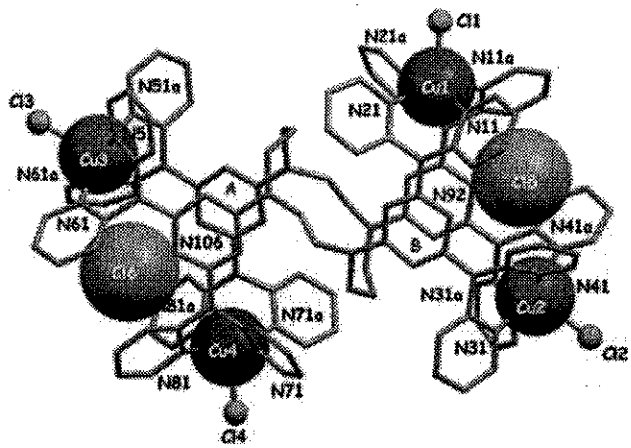

Figure 1. Representation of **1**, showing the four pentacoordinate Cu^{II} ions and the two encapsulated chloride anions Cl5 and Cl6.

Anion–π Interactions as Controlling Elements in Self-Assembly Reactions of Ag(I) Complexes with π-Acidic Aromatic Rings

Brandi L. Schottel,[†] Helen T. Chifotides,[†] Mikhail Shatruk,[†] Abdellatif Chouai,[†] Lisa M. Pérez,[†,§] John Bacsa,[†] and Kim R. Dunbar*[,†]

J. Am. Chem. Soc. **2006**, *128*, 5895.

3,6-bis(2'-pyridyl)-1,2,4,5-tetrazine

bptz

with $AgPF_6$

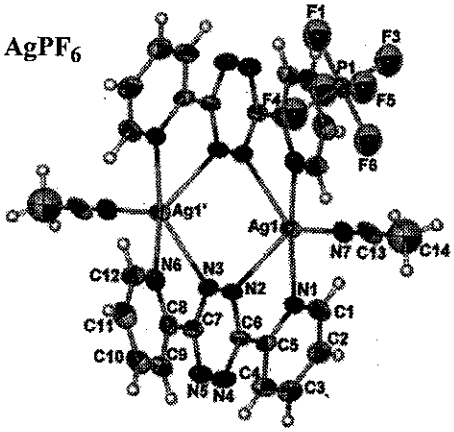

Figure 3. Thermal ellipsoid plot of $[Ag_2(bptz)_2(CH_3CN)_2][PF_6]_2$ (2) at the 50% probability level (one $[PF_6]^-$ ion has been omitted for clarity). The methyl carbon atom ellipsoids (C14) are depicted at the 25% probability level for the sake of clarity. Selected bond distances (Å) and angles (°): Ag1–N1 2.376(6), Ag1–N2 2.517(6), Ag1–N7 2.256(6), Ag1'-N6 2.342-(6), Ag1–N3 2.580(6), N1–Ag1–N2 68.3(2), N7–Ag1–N1 108.3(2), N7–Ag1–N2 94.7(2), N6–Ag1'–N3 67.0(3).

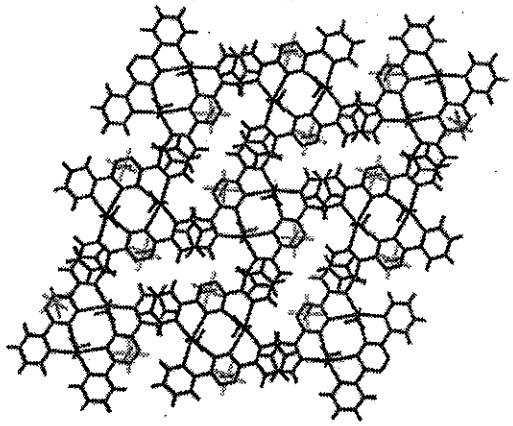

Figure 4. Packing diagram of $[Ag_2(bptz)_2(CH_3CN)_2][PF_6]_2$ (2) parallel to

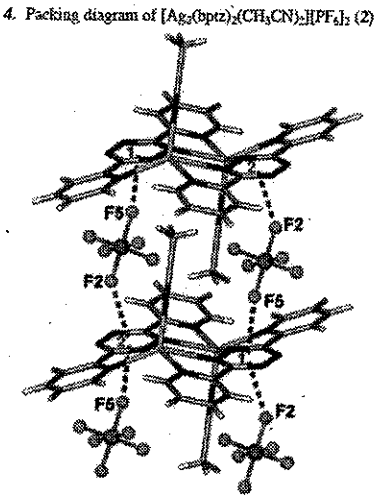

Figure 5. Portion of the crystal structure of $[Ag_2(bptz)_2(CH_3CN)_2][PF_6]_2$ (2) depicting the cation/anion arrangement and the shortest contacts between the $[PF_6]^-$ anions and the tetrazine ring centroids. Shortest F···tetrazine centroid distances (Å): centroid 1···F2 2.806(7), centroid 2···F5 2.835(7). The F···tetrazine plane distances are in the range 2.791–3.045 Å.

with $AgSbF_6$

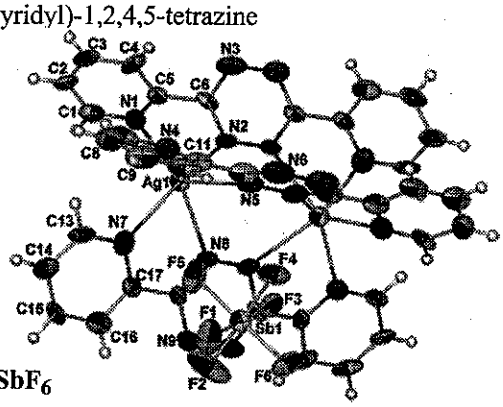

Figure 9. Thermal ellipsoid plot of $[Ag_2(bptz)_2][SbF_6]_2$ (5b) at the 50% probability level (one $[SbF_6]^-$ ion has been omitted for clarity). Selected bond distances (Å) and angles (°): Ag1–N1 2.438(3), Ag1–N2 2.554(3), Ag2–N3 2.575(3), Ag2–N6 2.434(3), N1–Ag1–N2 67.41(9), N3–Ag2–N6 66.19(9).

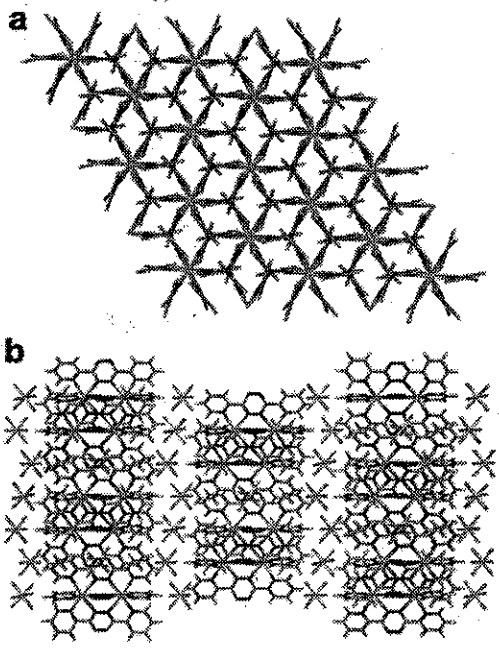

Figure 10. (a) Packing diagram of $[Ag_2(bptz)_2][SbF_6]_2$ (5b) along the *c* axis; (b) view perpendicular to the *c* axis.

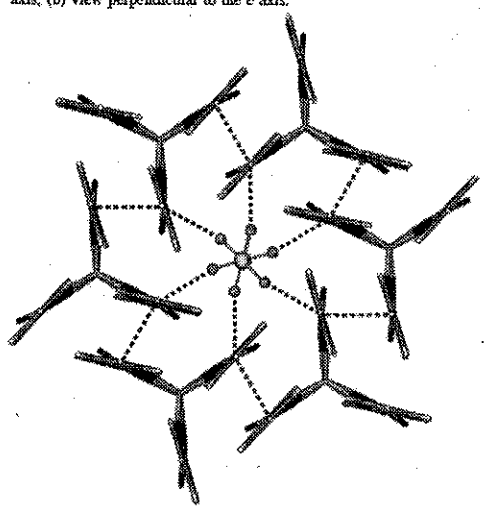

Figure 11. Anion–π interactions between a $[SbF_6]^-$ anion and six tetrazine rings in $[Ag_2(bptz)_2][SbF_6]_2$ (5b). The F–centroid distance is 3.265(3) Å (red dash lines); the F–tetrazine plane distance is 2.844 Å. The π–π contacts (3.36 Å) are indicated with purple dashed lines.

8/10

Ag : ligand = 1:1 で異なる配列

The aromatic ring must be electron deficient ?

Garau, C.; Quiñonero, D.; Frontera, A.; Ballester, P.; Costa, A.; Deyà, P.M. *New J. Chem.* **2003**, *27*, 211.

So far, examples are between anion and electron deficient aromatic rings. Anion-π interactions are possible between anions/lone pairs and the π cloud of non-electron-deficient aromatic molecules??

This is achieved whenever the aromatic ring is simultaneously interacting with a cation via the opposite face of the ring.

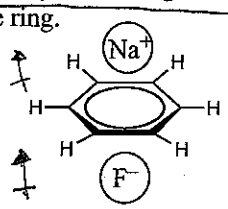

$r_{(Na^+-\pi)} = 2.4$ Å

$r_{(F^--\pi)} = 2.3$ Å

Table 3 Contributions to the total interaction energy (kcal mol^{-1}) calculated for $Na^+ \cdots$ benzene complex interacting with F^- at several distances (Å) from the center of the ring using MIPp

Distance	E_c	E_p	E_{ew}	E_t
1.5	−105.03	−64.38	99.68	−69.73
2.0	−90.74	−40.68	8.13	−123.28
2.5	−82.46	−25.90	−0.46	−108.83
3.0	−75.95	−17.15	−0.77	−93.87
3.5	−70.23	−11.93	−0.47	−82.63

76 fragments where noncovalent π interactions are present between lone pair electrons of electronegative atoms and benzene derivatives int eracting with a cation by the opposite face of the ring.

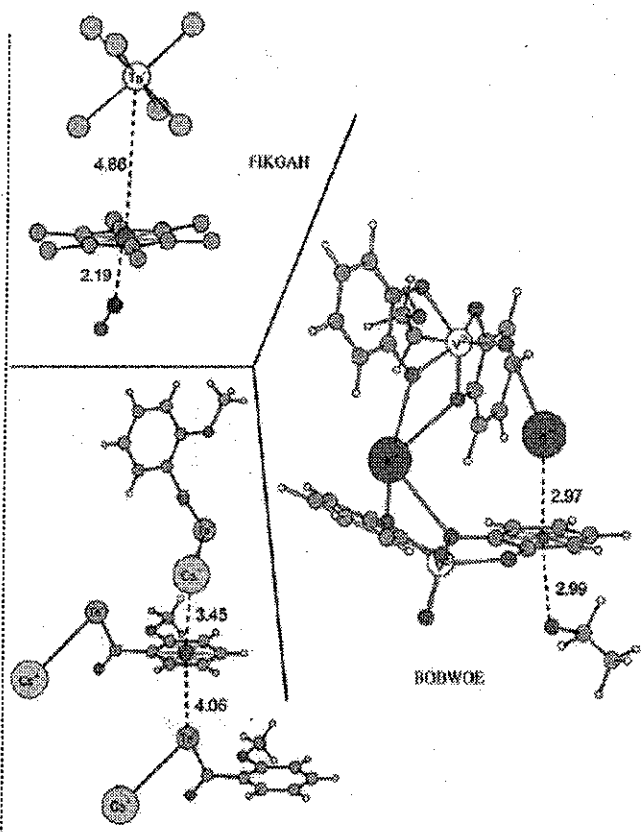

Fig. 4 X-Ray crystal structures of hexamethylbenzene nitrosyl hexachlorotantalum (FIKGAH),[29] dipotassium bis(catecholato)oxovanadium(IV) ethanol solvate monohydrate (BOBWOE)[30] and caesium 2-methoxybenzenecarbotelluroate (ZONKUI).[31]

J. Am. Chem. Soc. **1997**, *119*, 6324.

Anion Binding within the Cavity of π-Metalated Calixarenes

Mara Staffilani,† Kirsty S. B. Hancock,† Jonathan W. Steed,*,† K. Travis Holman,‡ Jerry L. Atwood,*,‡ Ravindra K. Juneja,§ and Robert S. Burkhalter§

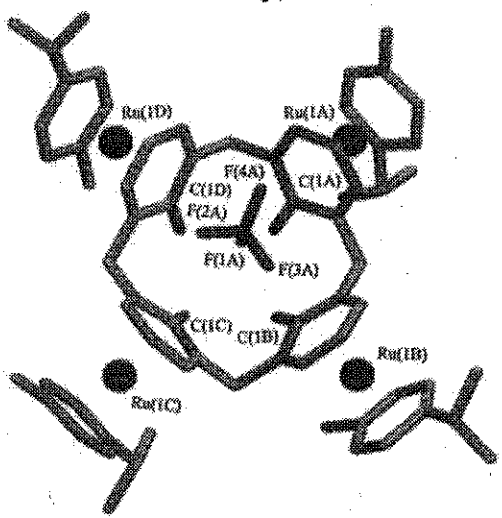

Figure 4. X-ray crystal structure of the tetrametallic complex **15a** showing the included BF_4^- anion. Shortest anion−host contacts F(1A)···C(1A), C(1D), C(1B), and C(1C) are 2.85, 2.87, 3.06, and 3.11 Å, respectively.

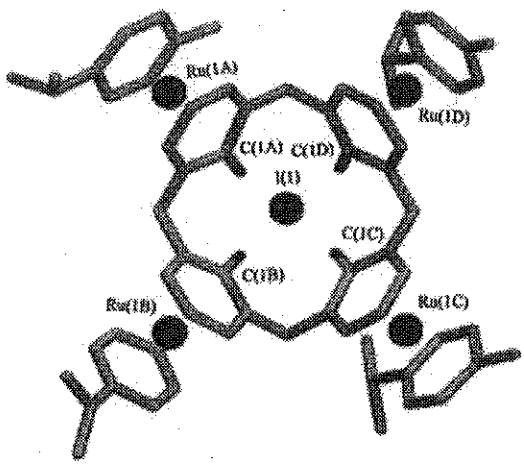

Figure 5. X-ray crystal structure of the tetrametallic complex **15d** showing the included I^- anion. Anion−calixarene ring centroid contacts I(1)···Cn(D), Cn(A), Cn(C), and Cn(B) are 3.60, 3.72, 3.73, and 3.78 Å, respectively.

Ter Steed, J.W.; Juneja, R.K.; Atwood, J.L. *Angew. Chem. Int. Ed.* **1994**, *33*, 2456.

4. Applications

A tri-armed sulfonamide host for selective binding of chloride

Frank Hettche and Reinhard W. Hoffmann*

New J. Chem. **2003**, *27*, 172.

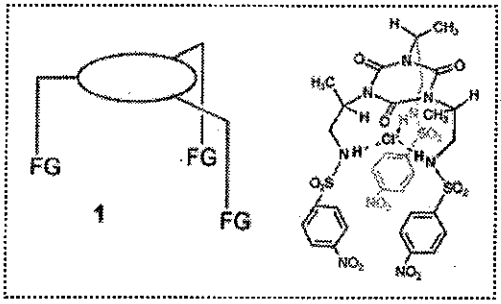

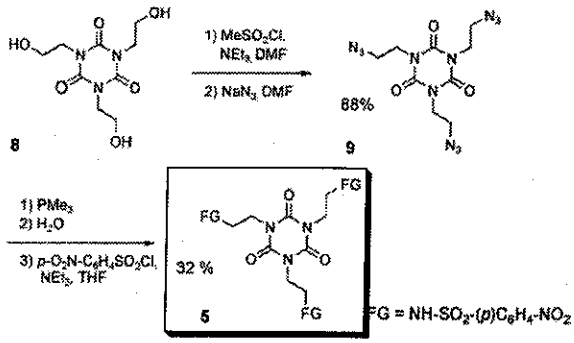

Scheme 3

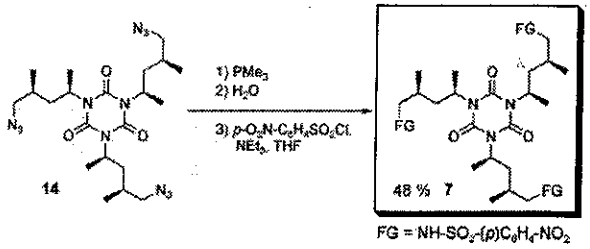

Scheme 5

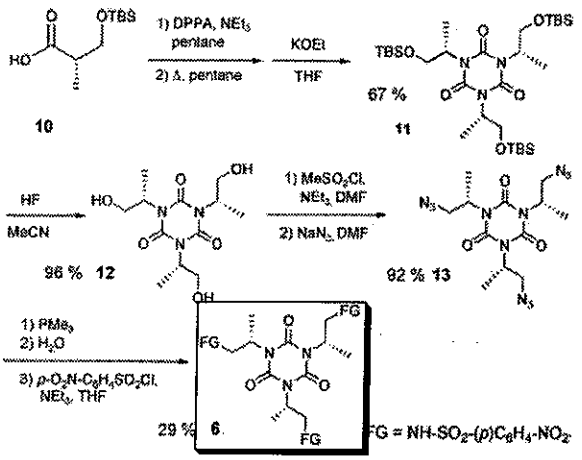

Scheme 4

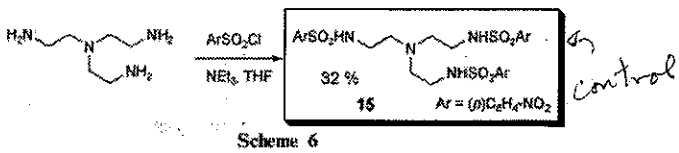

Scheme 6

Table 3 Binding constants for tetrabutylammonium salts in $CDCl_3$/DMSO 95:5 (300 K)

	Host			
Guest	7	5	6	15
Cl^-	4170 ± 130	4870 ± 170	12630 ± 1100	174 ± 5
Br^-	570 ± 30	1020 ± 65	425 ± 10	35 ± 5
NO_3^-	275 ± 10	380 ± 5	120 ± 10	< 10

Anion–π Interactions in Cyanuric Acids: A Combined Crystallographic and Computational Study

Antonio Frontera,*[a] Franciszek Saczewski,*[b] Maria Gdaniec,[c] Ewa Dziemidowicz-Borys,[b] Aleksandra Kurland,[b] Pere M. Deyà,* David Quiñonero,[a] and Carolina Garau[a]

Chem. Eur. J. **2005**, *11*, 6560.

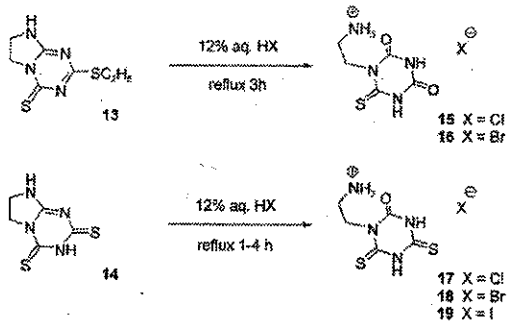

Scheme 1. Synthesis of halide salts **15–19**.

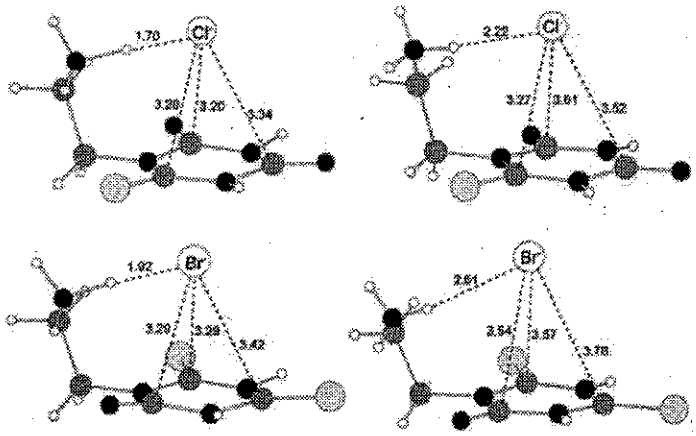

Figure 6. MP2(full)/6–31++G** optimized structures of **15** and **18** (left) and the corresponding experimental geometries obtained by X-ray crystallography (right). Distances are in Å.